Progress In Electromagnetics Research, Vol. 159, 15–26, 2017

A Compact CPW Fed CRR Loaded Four Element Metamaterial Array Antenna for Wireless Application

Naveen Mishra and Raghvendra Kumar Chaudhary*

Abstract—A compact coplanar waveguide (CPW) fed close ring resonator (CRR) loaded four-element metamaterial (MTM) array antenna for wireless application is designed and discussed in this article. The array is designed with corporate feeding network, arranged in a manner to offer 3 dB power at its each element. The proposed 1×4 MTM array antenna offers a fractional bandwidth of 10.18% with respect to the resonance frequency of $f_r = 2.26$ GHz. At the resonance frequency of 2.26 GHz, the proposed 1×4 MTM array antenna offers a gain of 5.10 dBi in the direction of broadside radiation. Each element of the proposed array antenna consists of CRR, which removes the requirement of via and allows the design of a uniplanar MTM array. The overall electrical size of the single element antenna shows compactness of $0.255\lambda_0 \times 0.155\lambda_0 \times 0.012\lambda_0$, where λ_0 is the free space wavelength at its resonance frequency of $f_r = 2.3$ GHz. The proposed MTM array antenna is designed and simulated on ANSYS HFSS 14.0, and simulated results are verified with the fabricated proto-type.

1. INTRODUCTION

In the last decade, there has been tremendous growth in the wireless communication when compact and high gain antennas are one of the key components. Because of unconventional properties such as negative permittivity and permeability, metamaterial (MTM) antennas are a well suited alternative to meet the demand for miniaturized antennas [1–3]. These MTM antennas are based on the concept of composite right- and left-handed, epsilon negative and mu negative transmission lines [4–10]. Although these antennas are miniaturized in nature, it faces a problem of narrow bandwidth [11, 12], poor gain and radiation efficiency [13, 14]. In the last few years, several works have been outlined, which claim the improvement in bandwidth and radiation efficiency [15–19]. In [16], a close ring resonator (CRR) is applied to design a dual-band MTM antenna. Ref. [17] presents a new aspect for bandwidth enhancement with the use of array of mushroom MTM structure. Further, bandwidth enhancement is achieved by forming an array of left-handed material unit cell and utilizing the left-handed material's concept of phase compensation and coupled resonance [18]. Besides [18] wideband property, this MTM array antenna suffers from the problem of negative gain. Miniaturization of MTM antennas restricts its gain to lower values. MTM antennas can overcome this restriction by using leaky wave antenna [19], EBG antenna [20] or array antenna [21–23] techniques similar to microstrip antennas [24]. In [21], broad bandwidth and high gain are achieved by using 3×2 and 3×3 U-slot array antennas. Another U-slot based single layered wideband high gain 2×2 array antenna is presented in [22]. A proximity coupled microstrip array antenna for bandwidth and gain enhancement is presented in [23]. Proximity coupling with air gap is used for bandwidth enhancement while array formation is done to achieve higher gain. Besides wideband and high gain properties, microstrip array antennas face a problem of large footprint area [21, 22]. Traditionally, microstrip array antenna uses T-junction for the feeding

Received 13 February 2017, Accepted 24 April 2017, Scheduled 11 May 2017

* Corresponding author: Raghvendra Kumar Chaudhary (raghvendra.chaudhary@gmail.com).
The authors are with the Department of Electronics Engineering, Indian Institute of Technology (Indian School of Mines), Dhanbad-826004, India.

network [22, 23, 25, 26]. In order to reduce the size of an array antenna, [26] introduced parasitically coupled feeding to the array and compared its performance with the conventional microstrip direct feeding technique. Parasitically coupled feeding shows considerable compactness without affecting the impedance bandwidth and gain in broadside direction. Further, to miniaturize the feed network of an array antenna, an MTM based T-junction power divider is designed in [27], which consists of a series gap and via responsible for generating left-handed capacitance and inductance, respectively.

This article presents a compact CPW-fed CRR loaded four-element MTM array antenna for wireless application. The investigation of array antenna starts from single element MTM antenna design, and further this single element antenna is attached with the 1×4 feeding network. Array antenna is designed with the CPW feeding technique and CRR which eliminate the requirement of via and allows a uniplanar and simple MTM array antenna. The proposed 1×4 MTM array antenna offers an impedance bandwidth of 10.18% and broadside gain of 5.10 dBi at the resonance frequency of 2.26 GHz.

2. SINGLE ELEMENT METAMATERIAL ANTENNA

Design process of the MTM array antenna initializes with the modelling of a single element MTM antenna. The proposed MTM antenna is composed of two series gaps within the patch and a CRR. These two series gaps are used to improve the desired working band of proposed MTM unit cell. The antenna is designed with the CPW feeding technique. Fig. 1 shows the layout of the proposed single element antenna, which is modelled on an FR-4 Substrate ($\varepsilon_r = 4.4$, $\tan\delta = 0.02$) with thickness 1.6 mm. The overall footprint size of the proposed single element antenna is $0.255\lambda_0 \times 0.155\lambda_0 \times 0.012\lambda_0$.

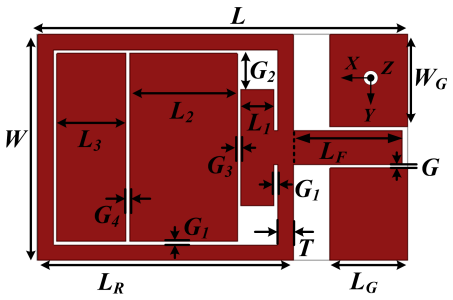

Figure 1. Layout of proposed single element MTM antenna. [All dimensions are in mm: $L = 33.30$, $L_F = 9.8$, $L_G = 7$, $L_R = 22.92$, $L_1 = 3$, $L_2 = 9.68$, $L_3 = 6.2$, $W = 20.22$, $W_G = 8.27$, $G = 0.31$, $G_1 = 0.31$, $G_2 = 3.51$, $G_3 = 0.31$, $G_4 = 0.31$, $T = 1.4$].

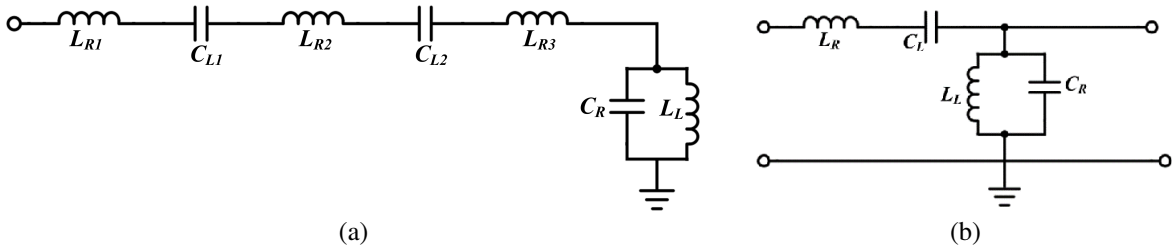

Figure 2. Equivalent circuit diagram. (a) Proposed single element MTM antenna. (b) Conventional CRLH-TL.

2.1. Equivalent Circuit Modelling

The equivalent circuit diagram of the proposed single element MTM antenna, which is similar to conventional composite right- and left-handed transmission line (CRLH-TL), is shown in Fig. 2. It consists of a pair of series and shunt lumped elements. In the proposed MTM structure, series lumped

elements, i.e., left-handed capacitance (C_{L1}, C_{L2}) and right-handed inductance (L_{R1}, L_{R2}, L_{R3}), are associated with the two series gaps inside the patch and the patch itself, respectively. CRR plays a role for left-handed inductance (L_L), and the separation between CRR and patch is responsible for offering right-handed capacitance (C_R). Hence metamaterial property could be understood by observing Fig. 2(a) and its resemblance with Fig. 2(b). Since the equivalent circuit diagram of the proposed single element antenna is similar to the equivalent circuit diagram of the CRLH-TL, the dispersion relation can be computed with the help of Bloch-Floquet theorem.

$$\beta(\omega)a = \cos^{-1}\left(1 + \frac{Z_{sea}(\omega)Y_{sha}(\omega)}{2}\right) \tag{1}$$

$$Z_{sea}(\omega) = j\left(\omega L_R - \frac{1}{\omega C_L}\right) \quad Y_{sha}(\omega) = j\left(\omega C_R - \frac{1}{\omega L_L}\right) \tag{2}$$

where Z_{sea} indicates the impedance of series arm and Z_{sha} the admittance of the shunt arm of the equivalent circuit diagram of the CRLH-TL.

Further, the dispersion relation can be simplified by putting the values of Eq. (2) in Eq. (1).

$$\beta(\omega)a = \cos^{-1}\left(1 - \frac{1}{2}\left(\frac{\omega^2}{\omega_R^2} - \frac{\omega_L^2}{\omega_{shunt}^2} - \frac{\omega_L^2}{\omega_{Series}^2} + \frac{\omega_L^2}{\omega^2}\right)\right) \tag{3}$$

where

$$\omega_{series} = \frac{1}{\sqrt{C_L L_R}}, \quad \omega_{shunt} = \frac{1}{\sqrt{C_R L_L}}, \quad \omega_L = \frac{1}{\sqrt{C_L L_L}}, \quad \omega_R = \frac{1}{\sqrt{C_R L_R}} \tag{4}$$

Further, the resonance mode of the proposed antenna can be calculated by ($\beta d = n\pi$) where n indicates the number of modes which may be 0, ±1, ±2, etc. In order to achieve the zeroth order resonance (ZOR) frequency, n should be 0, and the zeroth order resonance frequency can be concluded with associated inductance and capacitance values [28, 29].

2.2. Simulation Results and Discussion

2.2.1. Proof of Metamaterial

The comparison between input reflection coefficient plots of designed antenna with and without CRR is depicted in Fig. 3. It can be observed that the coupling of patches with CRR plays an important role for miniaturization of the proposed antenna by introducing a new band at the first resonance frequency ($f = 2.3$ GHz). Since the proposed antenna is designed with open-ended boundary condition, the shunt constraints of equivalent circuit play a vital role for the origination of ZOR in Eq. (1).

$$\omega_{Shunt} = \omega_{ZOR} = \frac{1}{\sqrt{L_L C_R}} \tag{5}$$

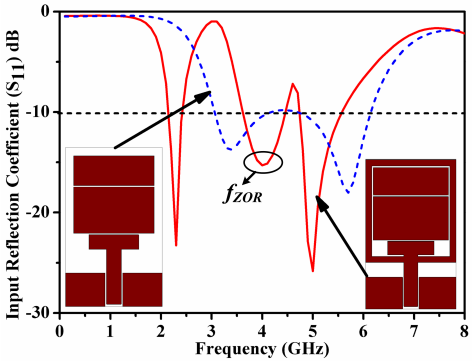

Figure 3. Comparison of input reflection coefficient of single element MTM antenna with and without CRR.

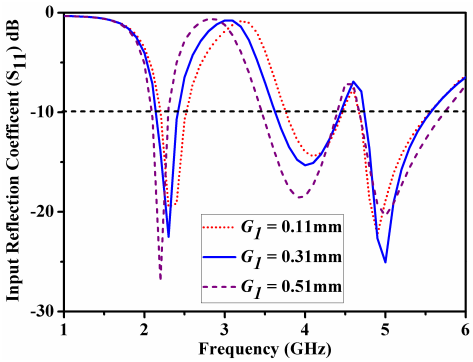

Figure 4. Input reflection coefficient plot for single element MTM antenna at various values of G_1.

Figure 4 depicts the input reflection coefficient plot of the proposed antenna at different values of gap G_1. It can be noticed that the increment in gap G_1 is responsible for the significant shift in the first and second (f_{ZOR}) resonance frequencies towards lower frequencies, while no significant variation is observed in the third resonance frequency. This shift in the first and second resonance frequencies towards lower frequencies is due to the increment in shunt inductance L_L. As gap G_1 increases, the thickness of CRR strip (T) decreases, which results in the increment of surface current density, hence L_L is increased [30].

Figure 5 shows vectored electric field distribution plots at all the three resonance frequencies. ZOR behaviour of the proposed antenna is well confirmed from Fig. 5(b). It can be observed that all the vectored electric field lines throughout the patch are perpendicular and in the same phase, hence ZOR [31]. Additionally Fig. 5(b) also conclude that the maximum electric field distribution at ZOR ($f_{ZOR} = 4$ GHz) frequency is between patches and CRR, while on other two resonance frequencies it is maximum on series as well as shunt parameters, Fig. 5(a) and Fig. 5(c). It clearly indicates that the other two resonance frequencies can be controlled by both series and shunt parameters.

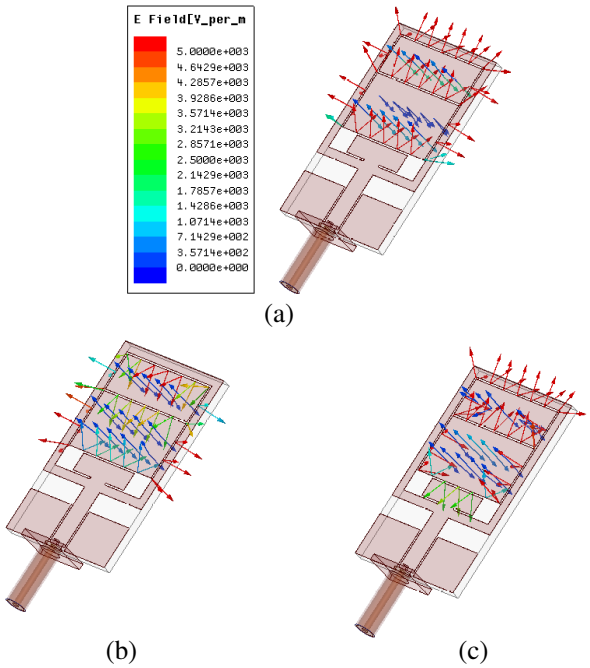

Figure 5. Electric filed distribution plot for proposed single element MTM antenna. (a) at 2.3 GHz, (b) at 4 GHz, (c) at 5 GHz.

Further, in order to verify the metamaterial property of the proposed antenna, unit cell analysis has been performed. Fig. 6 shows the dispersion diagram plot for the proposed antenna unit cell. It can be clearly observed that at the frequency of 4 GHz the value of βd becomes zero, hence ZOR [32–34]. In addition to the above, the dispersion diagram is divided in left-handed (LH) and right-handed (RH) regions. LH region indicates the range of frequency where the slope of the curve is negative, and it also indicates antiparallel phase and group velocity. On the other hand, the RH region is associated with the frequency range where slope of the curve is positive, and it also indicates parallel phase and group velocity. In the case of short-ended boundary conditions, the series constituent parameters (series capacitance and inductance and for open ended boundary conditions the shunt constituent parameters (shunt capacitance and inductance) define the ZOR frequency.

Figure 7 shows 3D polar plots at all the three resonance frequencies of single element MTM antenna. It clearly shows that the proposed MTM antenna has broadside gains of 2.13 dBi, 3.02 dBi and 3.81 dBi at 2.3 GHz, 4 GHz and 5 GHz, respectively. Since the main purpose of MTM antennas is for miniaturization, further complete array analysis is carried out on the first resonance frequency of 2.3 GHz.

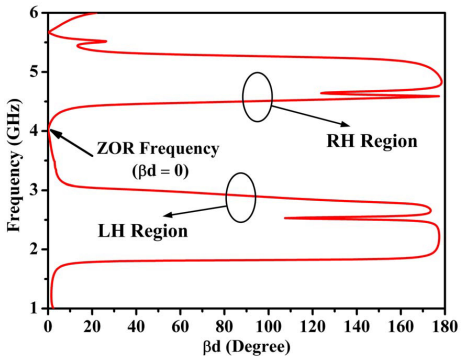

Figure 6. Dispersion diagram plot for the proposed antenna unit cell.

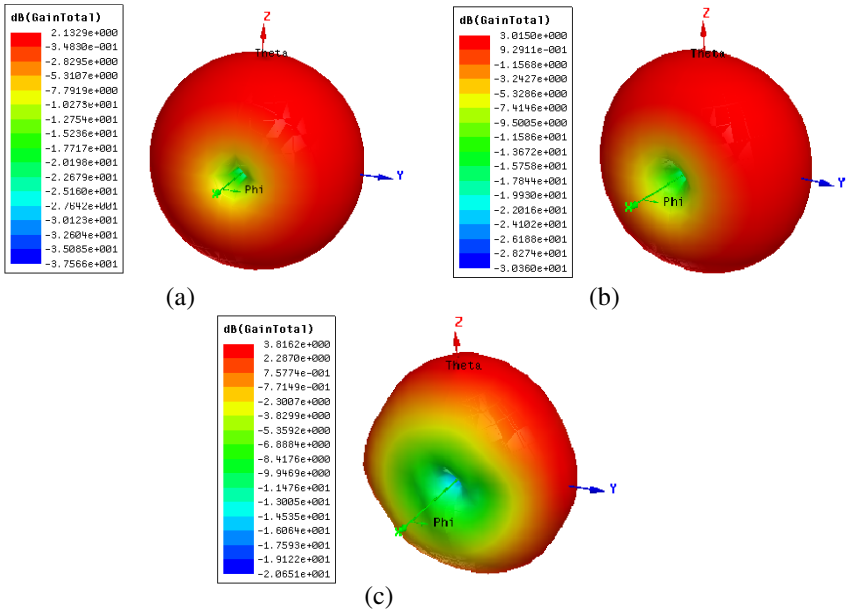

Figure 7. 3D polar plot at all the resonance frequencies of proposed single element MTM antenna. (a) at 2.3 GHz, (b) at 4 GHz, (c) at 5 GHz.

2.2.2. Analysis of First Resonance Frequency

Figure 8 shows the input reflection coefficient for different stages of the development of single element MTM antenna which is well explanatory. It is observed that the proposed single element antenna offers a −10 dB impedance bandwidth of 270 MHz (11.74% at $f_r = 2.3$ GHz) without compromising with the matching of antenna.

Figures 9(a) and (b) depict the simulated radiation pattern of the proposed structure in both xz- and yz-planes. At the resonance frequency of 2.3 GHz, the proposed antenna offers dipolar and omnidirectional radiation patterns in xz- and yz-planes, respectively. In addition to the above, it also offers consistent radiation pattern in both the planes (xz and yz) with cross-polarization levels of −63 dB and −51 dB, respectively in the maximum direction of radiation. The proposed single element antenna provides −3 dB beam width from −40.5° to 43° in xz-plane, and due to the omnidirectional radiation nature in yz-plane, −3 dB beam width cannot be measured. Fig. 10 depicts the simulated radiation efficiency and gain in the direction of broadside radiation. The proposed antenna structure offers an average broadside gain of 2.13 dBi and average radiation efficiency of 96% throughout the working band.

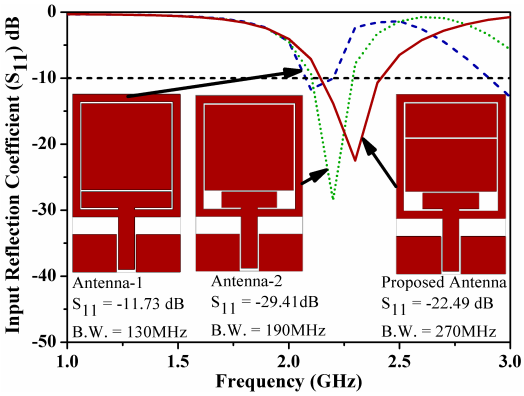

Figure 8. Input reflection coefficient for developing stages of proposed single element MTM antenna.

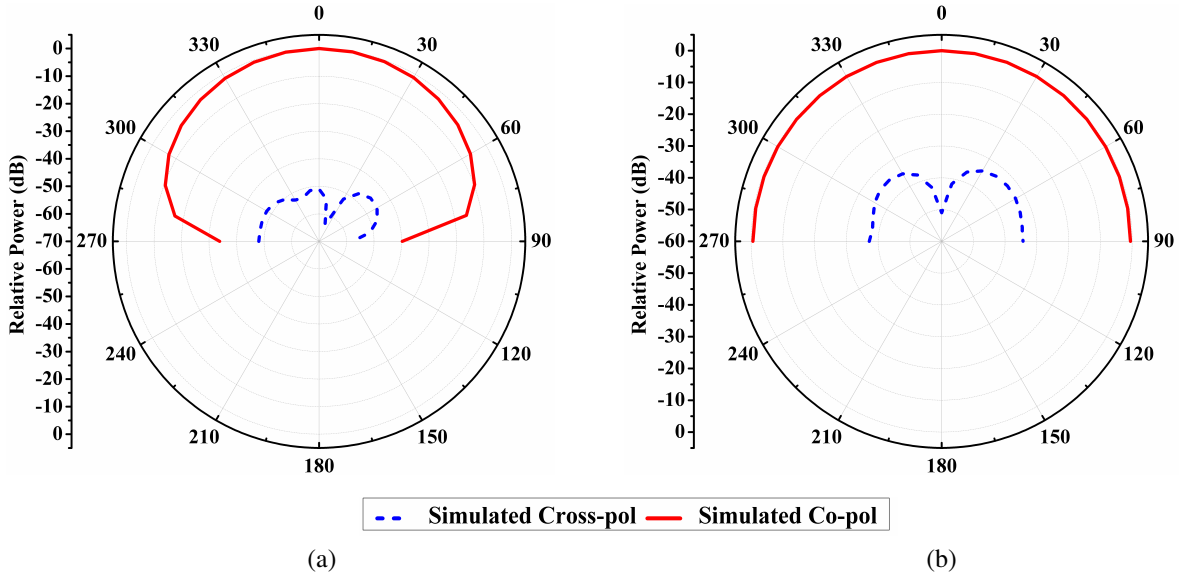

Figure 9. Simulated radiation pattern of proposed MTM antenna at 2.3 GHz. (a) xz-plane (b) yz-plane.

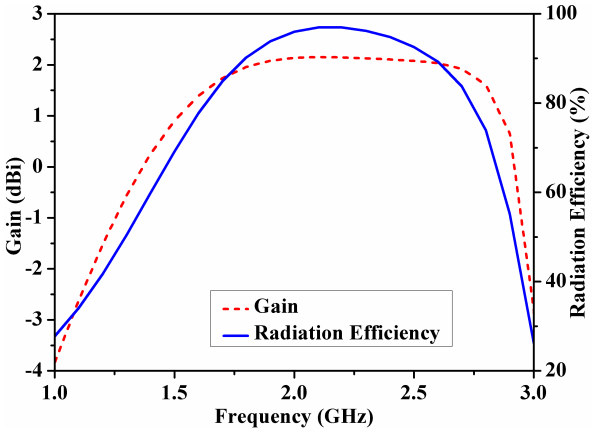

Figure 10. Simulated radiation efficiency and gain in broadside direction for the proposed MTM antenna.

3. 1 × 4 METAMATERIAL ARRAY ANTENNA

A corporate feed network based CPW-fed MTM array antenna for wireless applications is presented in this section. Feed network is designed in such a way so that it can offer 3 dB power at the input of its each element. Fig. 11 shows the input reflection coefficient plot for the power divider network. It can be clearly observed that the power divider network is not responsible for the origination of any resonance peak.

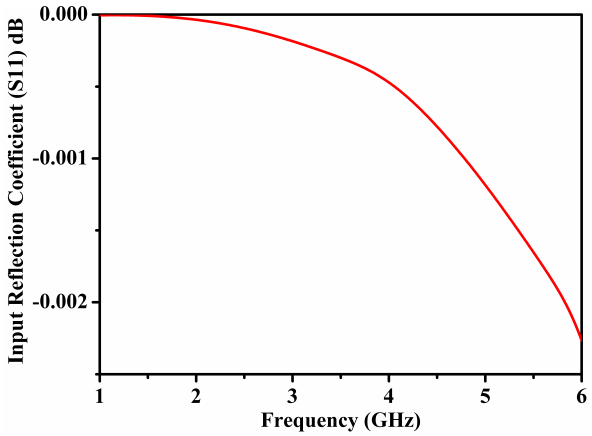

Figure 11. Input reflection coefficient curve for the power divider circuit.

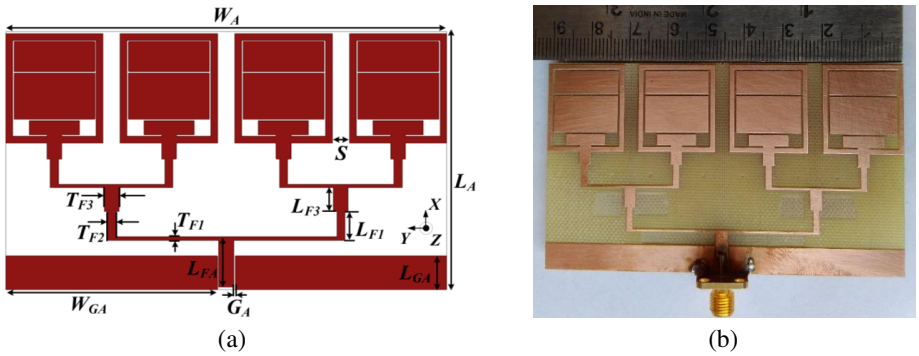

(a) (b)

Figure 12. 2D view of designed 1 × 4 MTM array antenna. All dimensions are in mm: $L_A = 53.93$, $L_{GA} = 7$, $L_{FA} = 9.8$, $L_{F1} = 6.01$, $L_{F3} = 5$, $S = 3.58$, $T_{F1} = 0.71$, $T_{F2} = 1.65$, $T_{F3} = 3.06$, $G_A = 0.31$, $W_A = 91.62$, $W_{GA} = 43.97$. (a) Layout of proposed array antenna. (b) Fabricated prototype of proposed array antenna.

Figure 12 shows the optimum 2-dimensional view of the proposed 1 × 4 MTM array antenna. Fig. 12(a) depicts the geometry of the proposed array antenna with feeding network parameters in caption. Fabricated prototype of the proposed 1 × 4 MTM array antenna is shown in Fig. 12(b). It is printed on an FR-4 substrate ($\varepsilon_r = 4.4$, $\tan\delta = 0.02$) of thickness 1.6 mm. The parameters of every element is the same as given for single element, and the electrical separation between elements of the array is $0.179\lambda_0$, where λ_0 is the free space wavelength at the resonant frequency of $f_r = 2.26$ GHz. Fig. 13 shows the measured and simulated input reflection coefficient plots for the proposed 1 × 4 array antenna. A good agreement is observed between measured and simulated input reflection coefficient plots. The slight change observed between measured and simulated ones is similar to that discussed in previous section. The proposed array antenna offers simulated and measured fractional bandwidths of 10.18% and 12% centred at 2.26 and 2.34 GHz, respectively.

Simulated and measured radiation patterns of the proposed array antenna at 2.26 GHz are shown in Figs. 14(a) and (b). They offer −29 dB and −36 dB simulated cross polarization level in the two

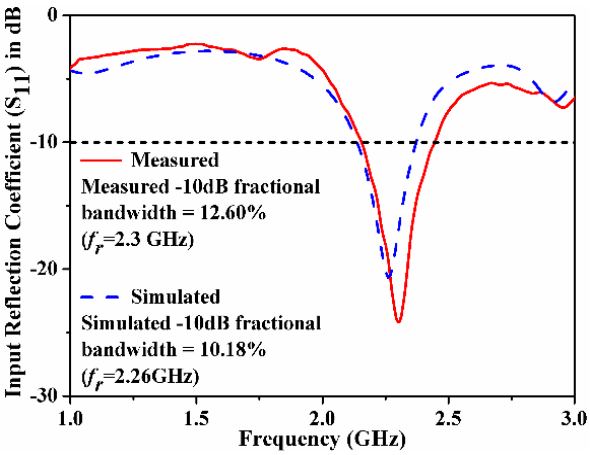

Figure 13. Measured and simulated input reflection coefficient of proposed MTM array antenna.

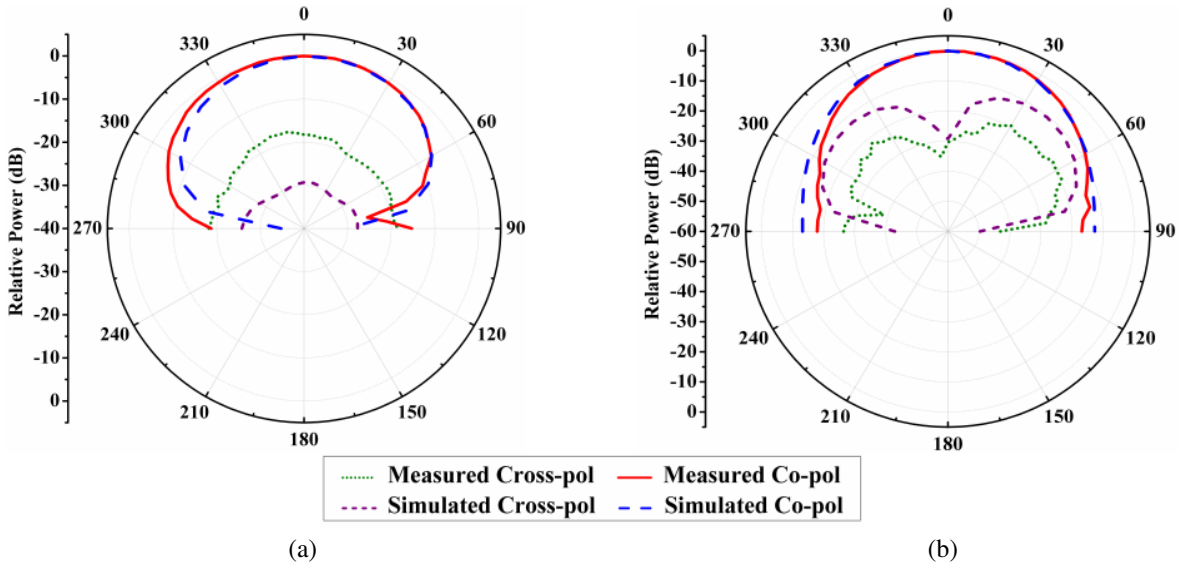

Figure 14. Simulated and measured radiation pattern of the proposed array antenna at 2.26 GHz. (a) xz-plane, (b) yz-plane.

planes respectively, in the maximum direction of radiation. It is clearly shown that the simulated −3 dB beamwidth of the proposed 1 × 4 array antenna lies from −38° to 44° and −33° to 34° in xz- and yz-planes respectively.

Figure 15 depicts the surface current distribution plot on the array structure at the frequency of 2.26 GHz. It can be clearly observed that the maximum surface current density mainly focuses on CRR, so the CRR plays a vital role for the radiation at 2.26 GHz frequency. Fig. 16 depicts the simulated and measured broadside gains along with the simulated radiation efficiency of 1 × 4 MTM array antenna. Throughout the complete working band, the proposed 1 × 4 MTM array antenna offers an average simulated and measured gains of 5.08 dBi and 5.04 dBi, respectively, in the direction of broadside radiation. In addition to the above, the proposed 1 × 4 array antenna offers an average radiation efficiency of 95.42% in the complete working band (2.14–2.37 GHz).

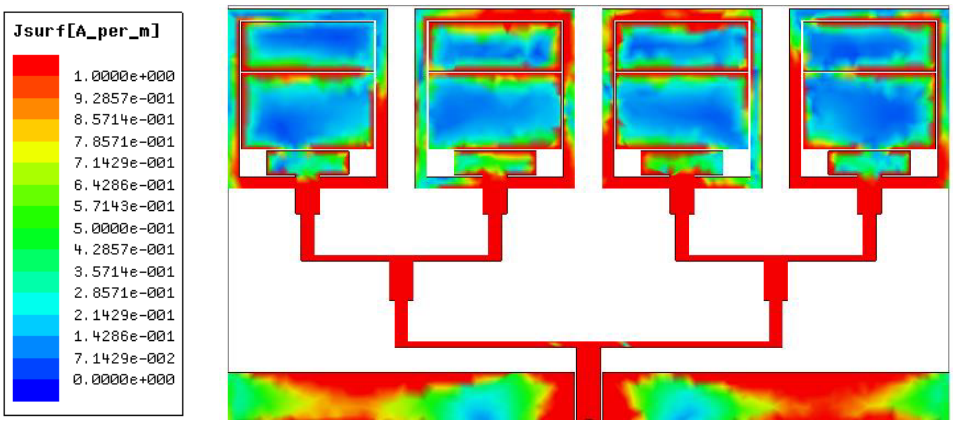

Figure 15. Surface current distribution plot on the proposed antenna array structure at 2.26 GHz frequency.

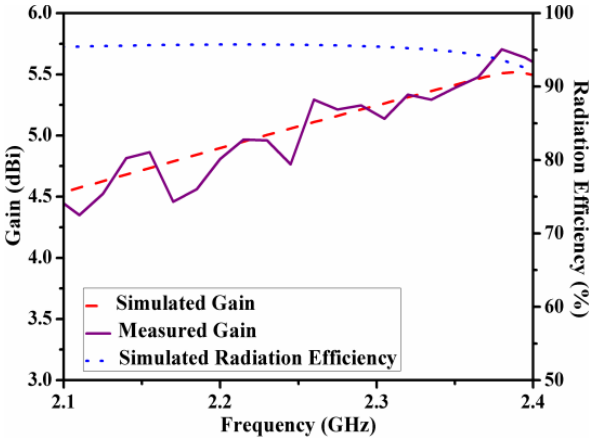

Figure 16. Simulated and measured broadside gain with simulated radiation efficiency of the proposed 1×4 array antenna.

4. PERFORMANCE OF PROPOSED ARRAY ANTENNA AND ITS COMPARISON

Table 1 compares the performance of the proposed 1×4 MTM array antenna with single element MTM antenna. It can be clearly seen that the proposed 1×4 array antenna offers good reasonable gain without compromising much with the impedance bandwidth and radiation efficiency. Additionally, 1×4 array antenna provides better -3 dB beamwidth in yz-plane than the single element MTM antenna, and in xz-plane it offers almost equal -3 dB beamwidth. Cross-polarization levels for all the three antennas are better than -20 dB and acceptable.

Table 2 shows the comparison of this work with the conventional microstrip array antenna and a published article. In order to design a conventional microstrip array antenna of the same size as 1×4 MTM array antenna, the MTM patch is replaced by a simple patch of the same size and equal element spacing. Feeding network also remains same as 1×4 MTM array antenna except slight improvement in feeding length. This improvement is required for proper matching at resonance frequency. It can be observed that the electrical size of the proposed 1×4 MTM array antenna is the smallest in the Table 2 because of the MTM approach. Additionally, the proposed 1×4 MTM array antenna offers better impedance bandwidth and radiation efficiency without compromising with the broadside gain.

Table 1. Performance comparison at different stage of proposed MTM array antenna.

S. N.	Parameters	Single element MTM antenna	1×4 MTM Array Antenna
1.	Resonant frequency (f_r) in GHz	2.30	**2.26**
2.	Overall antenna Size (mm^2)	33.30×20.22	53.93×91.62
3.	Impedance bandwidth (%)	11.74	**10.18**
4.	Broadside gain (dBi)	2.13	**5.10**
5.	Radiation Efficiency (%)	96.21	**95.66**
6.	Maximum Cross pol. at f_r in xz-plane (dB)	-63	-29
7.	Maximum Cross pol. at f_r in yz-plane (dB)	-51	-36
8.	-3 dB beamwidth at f_r in xz-plane (Degree)	83.5 (-40.5 to 43)	82 (-38 to 44)
9.	-3 dB beamwidth at f_r in yz-plane (Degree)	NA	67 (-33 to 34)

Table 2. Comparison of the proposed work with conventional and earlier published MTM array antenna.

S. N.	Parameters	This work	Conventional microstrip array	Direct fed array [26]
1.	Resonant frequency (GHz)	2.26	2.92	5.45
2.	Antenna footprint (mm^2)	53.93×91.62 ($\mathbf{0.41\lambda_0 \times 0.69\lambda_0}$)	56.93×91.62 ($0.55\lambda_0 \times 0.89\lambda_0$)	72.9×93.4 ($1.83\lambda_0 \times 2.35\lambda_0$)
3.	Relative bandwidth (%)	**10.18**	2.05	8.26
4.	Broadside gain (dBi)	**5.10**	4.17	11.64
5.	Efficiency (%)	**95.66**	43.52	89.5
6.	No. of elements	1×4	1×4	2×2

5. CONCLUSION

A corporate feed network based compact CPW-fed CRR loaded four-element MTM array antenna for wireless applications is presented. The overall electrical size of the single element MTM antenna shows a compactness of $0.255\lambda_0 \times 0.155\lambda_0 \times 0.012\lambda_0$, where λ_0 is the free space wavelength at its resonance frequency of $f_r = 2.3$ GHz. The resonator of MTM array consists of two series gaps inside the patch and CRR. Series gaps are inserted to achieve improved matching and bandwidth. The proposed 1×4 MTM array antenna offers 10.18% impedance bandwidth and broadside gain of 5.10 dBi at the resonant frequency of 2.26 GHz.

ACKNOWLEDGMENT

The authors want to show their sincere gratitude to Dr. K. V. Srivastava, Associate Professor Department of Electrical Engineering, IIT Kanpur, India, for offering the measurement facility for antenna prototype.

REFERENCES

1. Caloz, C. and T. Itoh, *Electromagnetic Metamaterials: Transmission Line Approach and Microwave Applications*, Wiley, Hoboken, NJ, 2005.
2. Ji, J. K., G. H. Kim, and W. M. Seong, "Bandwidth enhancement of metamaterial antennas based on composite right/left-handed transmission line," *IEEE Antennas Wireless Propag. Lett.*, Vol. 9, 36–39, 2010.
3. Sharma, S. K., A. Gupta, and R. K. Chaudhary, "Epsilon negative CPW-fed zeroth-order resonating antenna with backed ground plane for extended bandwidth and miniaturization," *IEEE Trans. on Antennas and Propagation*, Vol. 63, 5197–5203, 2015.
4. Mishra, N. and R. K. Chaudhary, "A miniaturized ZOR antenna with enhanced bandwidth for WiMAX applications," *Microwave and Optical Technology Lett.*, Vol. 58, 71–75, 2016.
5. Park, J. H., Y. H. Ryu, J. G. Lee, and J. H. Lee, "Epsilon negative zeroth order resonator antenna," *IEEE Trans. Antennas Propag.*, Vol. 55, 3710–3712, 2007.
6. Park, J. H., Y. H. Ryu, and J. H. Lee, "Mu zero resonance antenna," *IEEE Trans. Antennas Propag.*, Vol. 58, 1865–1875, 2010.
7. Upadhyaya, T. K., S. P. Kosta, R. Jyoti, and M. Palandoken, "Negative refractive index material inspired 900 electrically tilted ultra-wideband resonator," *Opt. Eng.*, Vol. 53, No. 10, 107104, Oct. 2014, DOI: 10.1117/1.OE.53.10.107104.
8. Upadhyaya, T. K., S. P. Kosta, R. Jyoti, and M. Palandöken, "Novel stacked μ-negative material-loaded antenna for satellite applications," *International Journal of Microwave and Wireless Technologies*, Vol. 8, No. 2, 229–235, Mar. 2016.
9. Xu, H.-X., G.-M. Wang, M.-Q. Qi, C.-X. Zhang, J.-G. Liang, J.-Q. Gong, and Y.-C. Zhou, "Analysis and design of two-dimensional resonant-type composite right left handed transmission lines with compact gain-enhanced resonant antennas," *IEEE Trans. Antennas Propag.*, Vol. 61, No. 2, 735–747, 2013.
10. Xu, H.-X., G.-M. Wang, Y.-Y. Lv, M.-Q. Qi, X. Gao, and S. Ge, "Multifrequency monopole antennas by loading metamaterial transmission lines with dual-shunt branch circuit," *Progress In Electromagnetics Research*, Vol. 137, 703–725, 2013.
11. Lee, H. M., "A compact zeroth-order resonant antenna employing novel composite right/left-handed transmission-line unit-cells structure," *IEEE Antennas Wireless Propag. Lett.*, Vol. 10, 1377–1380, 2011.
12. Lai, A., K. M. K. H. Leong, and T. Itoh, "Infinite wavelength resonant antennas with monopolar radiation pattern based on periodic structures," *IEEE Trans. Antennas Propag.*, Vol. 55, 868–876, 2007.
13. Liu, C. C., P. L. Chi, and Y. D. Lin, "Compact zeroth-order resonant antenna based on dual-arm spiral configuration," *IEEE Antennas Wireless Propag. Lett.*, Vol. 11, 318–321, 2012.
14. Mehdipour, A., T. A. Denidni, and A. Sebak, "Multi-band miniaturized antenna loaded by ZOR and CSRR metamaterial structures with monopolar radiation pattern," *IEEE Trans. Antennas Propag.*, Vol. 62, 555–562, 2014.
15. Mishra, N., A. Gupta, and R. K. Chaudhary, "A compact CPW-fed wideband metamaterial antenna using Ω-shaped interdigital capacitor for mobile applications," *Microwave and Optical Technology Lett.*, Vol. 57, 2558–2562, 2015.
16. Si, L.-M., W. Zhu, and H.-J. Sun, "A compact, planar, and CPW-fed metamaterial-inspired dual-band antenna," *IEEE Antenna Wireless Propag. Lett.*, Vol. 12, 305–308, 2013.

17. Liu, W., Z. N. Chen, and X. Qing, "Metamaterial-based low-profile broadband mushroom antenna," *IEEE Trans. on Antennas and Propag.*, Vol. 62, 1165–1172, 2014.
18. Palandoken, M., A. Grede, and H. Henke, "Broadband microstrip antenna with left-handed metamaterials," *IEEE Trans. on Antennas and Propag.*, Vol. 57, 331–338, 2009.
19. Nasimuddin, Z., N. Chen, and X. Qing, "Substrate integrated metamaterial-based leaky-wave antenna with improved boresight radiation bandwidth," *IEEE Trans. on Antennas and Propag.*, Vol. 61, 3451–3456, 2013.
20. Sedghi, M. S., M. Naser-Moghadasi, and F. B. Zarrabi, "Microstrip antenna miniaturization with fractal EBG and SRR loads for linear and circular polarizations," *International Journal of Microwave and Wireless Technologies*, 1–11, 2016.
21. Chen, H.-D., C.-Y.-D. Sim, J. Y. Wu, and T.-W. Chiu, Broadband high-gain microstrip array antennas for WiMAX base station," *IEEE Trans. on Antennas and Propag.*, Vol. 60, 3977–3980, 2012.
22. Wang, H., X. B. Huang, and D. G. Fang, A single layer wideband U-slot microstrip patch antenna array," *IEEE Antenna Wireless Propag. Lett.*, Vol. 7, 9–12, 2008.
23. Sharma, P. and S. Gupta, Bandwidth and gain enhancement in microstrip antenna array for 8 GHz frequency applications," *2014 Students Conference on Proc. Engineering and Systems (SCES)*, 1–6, Allahabad, India, May 2014.
24. Palandöken, M., "Microstrip antenna with compact anti-spiral slot resonator for 2.4 GHz energy harvesting applications," *Microwave And Optical Technology Letters*, Vol. 58, No. 6, 1404–1408, June 2016, DOI: 10.1002/mop.29824.
25. Levine, E., G. Malamud, S. Shtrikman, and D. Treves, "A study of microstrip array antennas with the feed network," *IEEE Trans. Antennas Propag.*, Vol. 37, 426–434, 1989.
26. Yeung, S. H., A. G. Lamperez, T. K. Sarkar, and M. S. Palma, "Comparison of the performance between a parasitically coupled and a direct coupled feed for a microstrip antenna array," *IEEE Trans. Antennas Propag.*, Vol. 62, 2813–2818, 2014.
27. Raheem, A. and E. K. I. Hamad, "Design of compact-efficient array of patch based on metamaterial T-junction," *Proc. IEEE APS, (MECAP)*, 1–3, Cairo, Egypt, 2010.
28. Mansouri, Z., A. S. Arezoomand, S. Heydari, and F. B. Zarrabi, "Dual notch UWB fork monopole antenna with CRLH metamaterial load," *Progress In Electromagnetics Research C*, Vol. 65, 111–119, 2016.
29. Lee, H. M., "A compact co-planar waveguide-fed zeroth-order resonant antenna with an improved efficiency and gain employing two symmetric unit cells," *Electrical and Electronic Engineering*, Vol. 1, No. 1, 12–16, 2011.
30. Kompa, G., *Practical Microstrip Design and Applications*, Artech House, London, 2005.
31. Jang, T., J. Choi, and S. Lim, "Compact coplanar waveguide (CPW)-fed zeroth-order resonant antennas with extended bandwidth and high efficiency on via-less single layer," *IEEE Trans. Antennas Propag.*, Vol. 59, 363–372, 2011.
32. Saravani, S., C. K. Chakrabarty, and N. Md Din, "Compact bandwidth-enhanced center-fed CPW zeroth-order resonant antenna loaded by parasitic element," *Progress In Electromagnetics Research Letters*, Vol. 66, 1–8, 2017.
33. Lee, J.-G., D.-J. Kim, and J.-H. Lee, "Compact penta-band dual ZOR antenna for mobile applications," *International Journal of Antennas and Propagation*, 2016.
34. Xiu, X. H., W. G.-Ming, and G. J.-Qiang, "Compact dual-band zeroth-order resonance antenna," *Chinese Physics Letters*, Vol. 29, No. 1, 014101, 2012.